Supporting Information

Lead-free, stable orange-red-emitting hybrid copper based organic-inorganic compounds

Le Wang, [†,‡] *Haochen Sun,* [§] *Chun Sun*,* [†,‡] *Da Xu,* [†,‡] *Jiaqi Tao,* [†,‡] *Tong Wei,*[†,‡] *Zi-hui Zhang,* [†,‡] *Yonghui Zhang,* [†,‡] *Ziying Wang,* [†,‡] *and Wengang Bi** [†,‡]

† State Key Laboratory of Reliability and Intelligence of Electrical Equipment, Hebei University of Technology, 5340 Xiping Road, Tianjin, 300401, P. R. China

‡ Tianjin Key Laboratory of Electronic Materials and Devices, School of Electronics and Information Engineering, Hebei University of Technology, 5340 Xiping Road, Tianjin, 300401, P. R. China

§ College of Materials Science and Engineering, Hebei University of Technology, 5340 Xiping Road, Tianjin, 300401, P. R. China

AUTHOR INFORMATION

Corresponding Author

*E-mail: cs@hebut.edu.cn (Chun Sun), wbi@hebut.edu.cn (Wengang Bi)

Experimental Section

Chemicals. Octadecene (90%, ODE) was obtained from Alfa Aesar. Oleic Acid (85%, OA) was purchased from TCI Shanghai. Cupric Acetate Anhydrous (99.99%, $Cu(OAC)_2$), Iodotrimethylsilane (97%, TMSI), Bromobenzene (99.5%), Copper iodide (98%, CuI), Phenylethylamine (98%, PEA), Polyvinylpyrrolidone (Mw= 58000, PVP) were purchased from Aladdin. Hexane (98%) was attained from Tianjin Chemical Factory. All the chemicals were used without further purification.

Growth of $(PEA)_4Cu_4I_4$ bulk crystals. 0.1mmol of CuI, 5μL of PEA were mixed and dissolved in 1mL bromobenzene to form a clear precursor solution. Bulk crystals were obtained by diffusing 10mL hexane into the 1mL precursor solution at room temperature for overnight in a glove box. The large crystals were washed with hexane.

Synthesis of $(PEA)_4Cu_4I_4$ by hot-injection method. 0.1mmol of $Cu(OAC)_2$, 1mL of OA, 5mL of ODE and 0.5mL of PEA were loaded into a 50 mL three-neck round-bottom flask. The solution was degassed by purging with N_2 at 120°C for 0.5h. Then, the flask was heated up to 180°C. After 0.1 mL of TMSI was injected, an ice-water bath was immediately applied. The as-prepared solution was subjected to centrifuge at 5000 rpm for 10 min. After that, hexane was added to wash the precipitates.

LED Fabrication. UV-LED chips with an emission peak wavelength centered at 365 nm were purchased from Epileds Technologies. A certain amount of $(PEA)_4Cu_4I_4$ powder was mixed with PVP/water solution and coated onto the UV-LED chip. Finally, this chip was dried under vacuum for 1 h.

Measurement and Characterization.

Single crystal X-ray diffraction (SCXRD).

SCXRD data of $(PEA)_4Cu_4I_4$ was performed on a BRUKER D8 VENTURE PHOTON II area-detector diffractometer with graphite-monochromated Mo Kα radiation (λ = 0.71073 Å) using ω-scan technique. SAINT program was used for the integration of diffraction data and the intensity correction for the Lorentz and polarization effects. Semi-empirical absorption corrections were applied using SADABS program. The structures were solved by direct methods and refined with the full-matrix least-squares technique based on F^2 using the SHELXL-97 program. All non-hydrogen atoms were refined anisotropically and all the hydrogen atoms were introduced at the calculated positions. The single crystal data have been recorded by the Cambridge Crystallographic Data Center (CCDC No: 2052835 and No: 2052838).

X-ray powder diffraction.

X-ray di□raction (XRD) patterns of $(PEA)_4Cu_4I_4$ powder were carried out by a Bruker D8 ADVANCE X-ray di□ractometer (Cu Kα: λ = 1.5406 Å). The diffraction patterns were scanned over the angular range of 5-60 degree (2θ) with a step size of 0.02, at room temperature. Simulated powder pattern was calculated by Mercury software using the crystallographic information file obtained from SCXRD experiment.

Fourier transform infrared (FTIR)

FTIR spectroscopy was recorded on a Thermo-Nicole iS50 FTIR spectrometer with attenuated total reflection detector.

Photoluminescence (PL) spectra and PL excitation (PLE) spectra

PL spectra and PL excitation PLE spectra were measured by a GANGDONG F-320 fluorescence spectrometer.

X-ray photoelectron spectroscopy (XPS)

XPS was performed on a Thermo Fisher K-Alpha spectrometer.

Absorbance spectra

Absorbance spectra of samples were measured by Shimadzu UV-3600

Photoluminescence quantum yield and Time-resolved photoluminescence.

The absolute PLQYs and time-resolved PL lifetime of the samples were measured by a fluorescence spectrometer (FLS920P, Edinburgh Instruments)

Material photostability study.

To test the photostability, a 12W UV analyzer is used as a continuous light source. The photoluminescence spectrum was measured by using an Ocean Optics spectrometer.

Table S1. Crystal data for $(PEA)_4Cu_4I_4$ at 293K.

Compound	$(PEA)_4Cu_4I_4$
Empirical formula	$C_{32} H_{44} Cu_4 I_4 N_4$
Formula weight	1246.47 g/mol
Temperature	293(2) K
Crystal system	Monoclinic
Space group	P 1 21/c 1
a	19.2933(12) Å
b	29.3326(18) Å
c	7.5241(5) Å
α	90 deg
β	94.005(2) deg
γ	90 deg
Volume	4247.7(5) $Å^3$
Z	4
Calculated density	1.949 Mg/m^3
Absorption coefficient	4.908 mm^{-1}
Theta range for data collection	2.970 to 27.558 deg
Reflections collected / unique	89620 / 9777 [R(int) = 0.1261]
Completeness to theta = 25.242	99.8 %
Max. and min. transmission	0.7456 and 0.5554
Data / restraints / parameters	9777 / 35 / 349
Final R indices [I>2sigma(I)]	R1 = 0.0825, wR2 = 0.1811
R indices (all data)	R1 = 0.1731, wR2 = 0.2130
Goodness-of-fit on F^2	1.071

Table S2. Bond lengths [Å] and angles [deg] for $(PEA)_4Cu_4I_4$ at 293K.

I(4)-Cu(4)	2.7090(19)
I(4)-Cu(2)	2.753(2)
I(4)-Cu(3)	2.6572(18)
I(1)-Cu(2)	2.6604(18)
I(1)-Cu(1)	2.7195(19)
I(1)-Cu(3)	2.720(2)
I(2)-Cu(4)	2.688(2)
I(2)-Cu(2)	2.7038(19)
I(2)-Cu(1)	2.7038(19)
I(3)-Cu(4)	2.694(2)
I(3)-Cu(1)	2.673(2)
I(3)-Cu(3)	2.754(2)
Cu(4)-Cu(2)	2.697(3)
Cu(4)-Cu(1)	2.671(2)
Cu(4)-Cu(3)	2.642(2)
Cu(4)-N(4)	2.022(10)

Cu(2)-Cu(1)	2.630(2)
Cu(2)-Cu(3)	2.703(3)
Cu(2)-N(2)	2.019(11)
Cu(1)-Cu(3)	2.704(2)
Cu(1)-N(1)	2.028(9)
Cu(3)-N(3)	2.028(9)
N(1)-H(1A)	0.89
N(1)-H(1B)	0.89
N(1)-C(8)	1.485(19)
N(3)-H(3A)	0.89
N(3)-H(3B)	0.89
N(3)-C(24)	1.62(2)
N(2)-H(2A)	0.89
N(2)-H(2B)	0.89
N(2)-C(16)	1.487(19)
C(32)-H(32A)	0.97
C(32)-H(32B)	0.97
C(32)-N(4)	1.445(17)
C(32)-C(31)	1.533(17)
N(4)-H(4A)	0.89
N(4)-H(4B)	0.89
C(30)-C(25)	1.39
C(30)-C(29)	1.39
C(30)-C(31)	1.492(16)
C(25)-H(25)	0.93
C(25)-C(26)	1.39
C(26)-H(26)	0.93
C(26)-C(27)	1.39
C(27)-H(27)	0.93
C(27)-C(28)	1.39
C(28)-H(28)	0.93
C(28)-C(29)	1.39
C(29)-H(29)	0.93
C(16)-H(16A)	0.97
C(16)-H(16B)	0.97
C(16)-C(15)	1.42(2)
C(8)-H(8A)	0.97
C(8)-H(8B)	0.97
C(8)-C(7)	1.44(2)
C(24)-H(24A)	0.97
C(24)-H(24B)	0.97
C(24)-C(23)	1.374(16)
C(7)-H(7A)	0.97
C(7)-H(7B)	0.97

C(7)-C(6)	1.539(19)
C(6)-C(5)	1.39
C(6)-C(1)	1.39
C(5)-H(5)	0.93
C(5)-C(4)	1.39
C(4)-H(4)	0.93
C(4)-C(3)	1.39
C(3)-H(3)	0.93
C(3)-C(2)	1.39
C(2)-H(2)	0.93
C(2)-C(1)	1.39
C(1)-H(1)	0.93
C(15)-H(15A)	0.97
C(15)-H(15B)	0.97
C(15)-C(14)	1.56(2)
C(23)-H(23A)	0.97
C(23)-H(23B)	0.97
C(23)-C(22)	1.71(3)
C(21)-H(21)	0.93
C(21)-C(20)	1.39
C(21)-C(22)	1.39
C(20)-H(20)	0.93
C(20)-C(19)	1.39
C(19)-H(19)	0.93
C(19)-C(18)	1.39
C(18)-H(18)	0.93
C(18)-C(17)	1.39
C(17)-H(17)	0.93
C(17)-C(22)	1.39
C(9)-H(9)	0.93
C(9)-C(14)	1.39
C(9)-C(10)	1.39
C(14)-C(13)	1.39
C(13)-H(13)	0.93
C(13)-C(12)	1.39
C(12)-H(12)	0.93
C(12)-C(11)	1.39
C(11)-H(11)	0.93
C(11)-C(10)	1.39
C(10)-H(10)	0.93
C(31)-H(31A)	0.97
C(31)-H(31B)	0.97

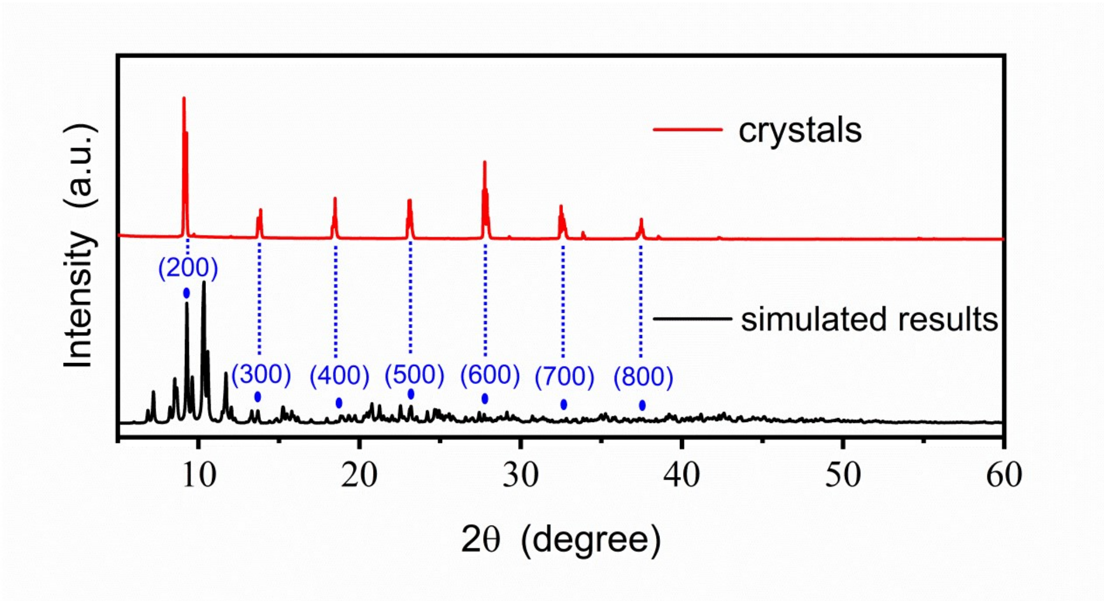

Figure S1. PXRD patterns of $(PEA)_4Cu_4I_4$ crystals as well as the software simulation results.

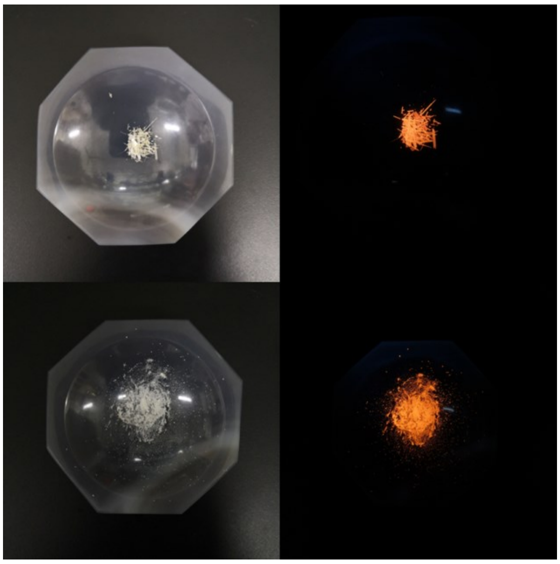

Figure S2. Images of $(PEA)_4Cu_4I_4$ crystals before (top) and after (bottom) grinding under ambient light and UV irradiation.

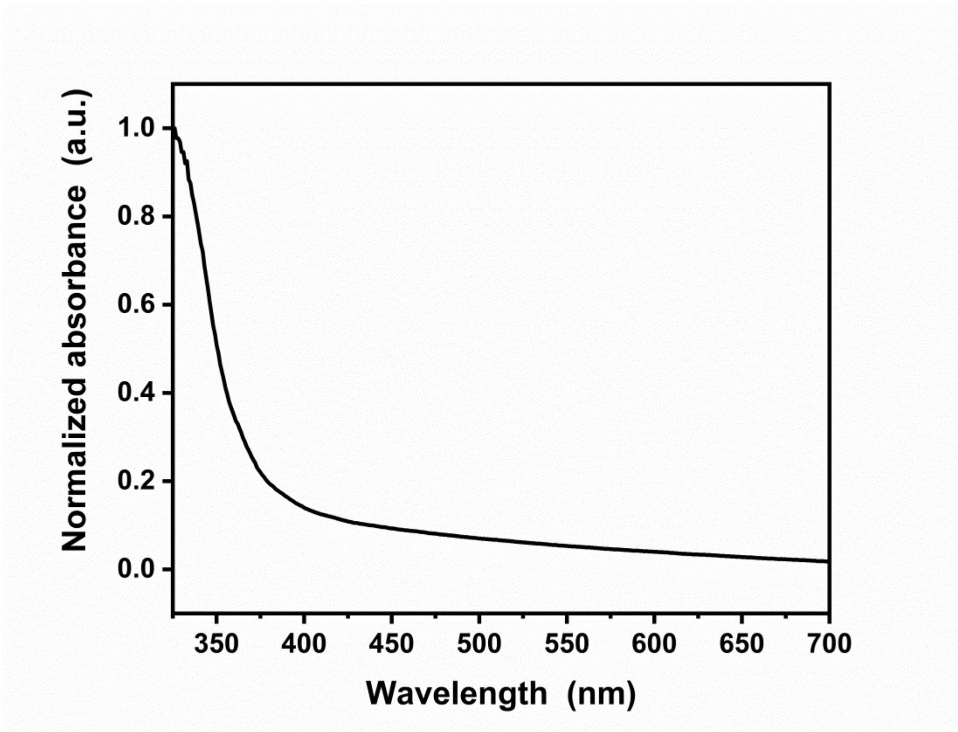

Figure S3. Absorption spectrum of $(PEA)_4Cu_4I_4$ crystals.

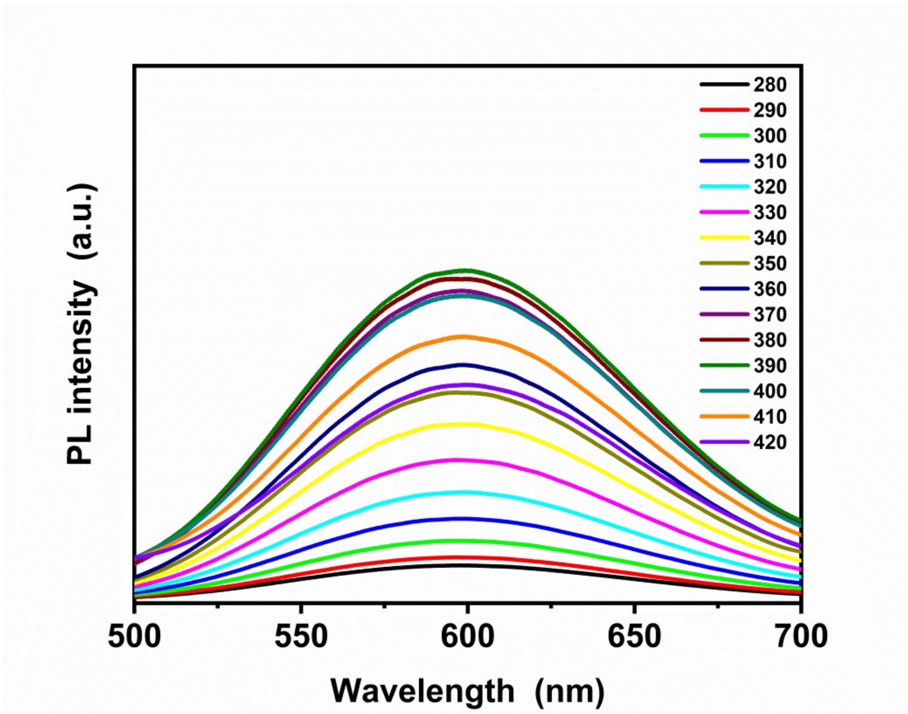

Figure S4. Emission spectra of $(PEA)_4Cu_4I_4$ crystals at different excitation wavelengths.

Table S3. Summary of emissive properties of Cu(I) complexes.

Compound	λem	QY	Reference
$Cu_4I_4(PPh_2(CH_2)_2Si(OCH_2CH_3)_3)_4$	598 nm	31 %	1
Cu_6(6-methyl-2-pyridinethiolato)$_6$	677 nm	10 %	2
$Cu_4I_4(PPh_2$-$(CH_2CH{=}CH_2))_4$	580 nm	14 %	3
Cu_4I_4(2-((diphenylphosphino)methyl)pyridine)$_2$	460/580 nm	43 %	4
$(CuI)_3$(bis(dicyclohexylphosphino)-methane)$_2$	626 nm	11 %	5
$(CuI)_4$(bis(dicyclohexylphosphino)-methane)$_2$	590 nm	12 %	5
$(Cu_3$(5-(pyridin-4-yl)-1H-1,2,4-triazole-3-thiol)$_3)_2\cdot$3(N,N-dimethylformamide)$\cdot 3H_2O$	904 nm	4.3 %	6
(Cu(5-(pyridin-4-yl)-1H-1,2,4-triazole-3-thiol))$_6\cdot$8(N,N-dimethylformamide)$\cdot 7H_2O$	776 nm	1.6 %	6
(2-(Diphenylphosphino)-5-phenyl-1,3,4-thiadiazole)$_4Cu_4I_4$	617 nm	45 %	7
Cu_6I_6(1,3-bis(diphenylphosphino)propane)$_3$	655 nm	39 %	8
CuI(2-cyano-pyridine)	618 nm	10 %	9
Cu_4I_4(3-benzyloxy-pyridine)$_4$	590 nm	86 %	10
Cu_4I_4(1-propyl-1H-benzo[d]imidazole)$_4$	600 nm	96 %	10
Cu_4I_4(1,3-propandiamine)$_2$	616 nm	65 %	10
Cu_4I_4(1,5-di(1H-imidazol-1-yl)pentane)$_2$	620 nm	64 %	10
Cu_4I_4(1,3-bis(4-pyridyl)propane)$_2$	613 nm	56 %	10
Cu_4I_4(1,4-butanediamine)$_2$	585 nm	61 %	10
Cu_4I_4(ethylenediamine)$_2$	590 nm	70 %	10
Cu_4I_4(diisopropyl-ether)$_2$	580 nm	66 %	10
Cu_2I_2(5-Methyl-pyrimidine)$_2$	570 nm	30.8%	11
Cu_2I_2(triphenylphosphine)$_2$(pyrazine)	631 nm	26.1%	11
Cu_2I_2(1-(3-(1H-benzo[d]imidazol-1-yl)propyl)-1H-benzo[d][1,2,3]triazole)$_2$	572 nm	56%	12
Cu_4I_6(3-(5-Fluoro-1H-benzo[d][1,2,3]triazol-1-yl)-N,N,N-trimethylpropan-1-aminium)$_2$	615 nm	53%	13
Cu_4I_6(3-(5-Methyl-1H-benzo[d][1,2,3]triazol-1-yl)-N,N,N-trimethylpropan-1-aminium)$_2$	596 nm	85%	13
phenethylamine(PEA)$_4Cu_4I_4$	598 nm	68%	Our work

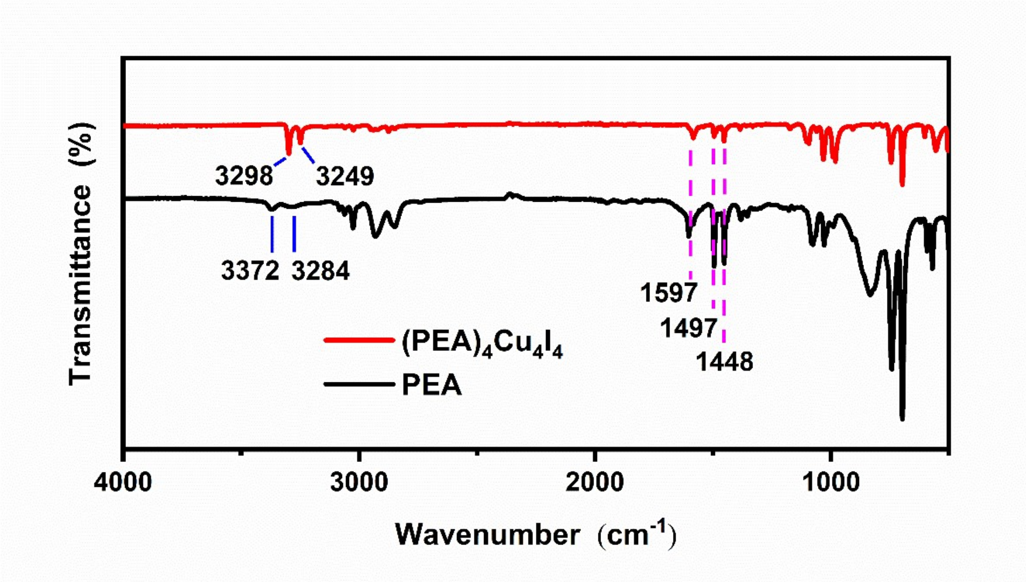

Figure S5. The FTIR spectra of $(PEA)_4Cu_4I_4$ crystals and PEA.

As shown in Figure S5, the three bands of 1448, 1497 and 1597 cm^{-1} observed for both the PEA and the crystals are assigned to the stretching vibration of C=C from benzene ring modes,[14] confirming the existence of PEA molecules in the crystals. The two bands observed at 3372 cm^{-1} and 3284 cm^{-1} for the PEA are assigned to the N-H stretching modes[14], and these bands are shifted to lower frequencies of 3298 cm^{-1} and 3249 cm^{-1} for the crystals, demonstrating that the amino groups coordinate with the Cu_4I_4 cluster.

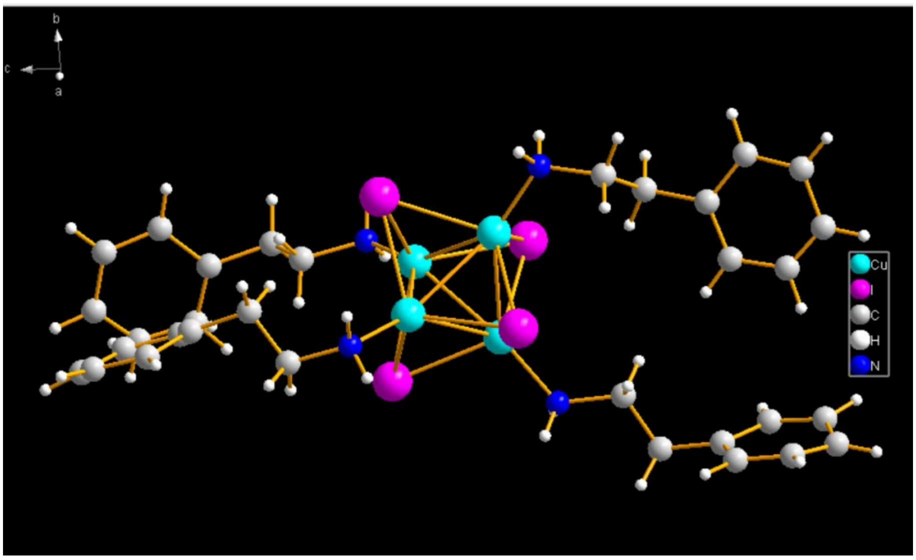

Figure S6. The structure of $(PEA)_4Cu_4I_4$ at 193 K.

Table S4. Crystal data for $(PEA)_4Cu_4I_4$ at 193K.

Compound	$(PEA)_4Cu_4I_4$
Empirical formula	C_{32} H_{44} Cu_4 I_4 N_4
Formula weight	1246.47 g/mol
Temperature	193(2) K
Crystal system	Monoclinic
Space group	C c
a	10.3866(9) Å
b	10.3829(9) Å
c	38.197(4) Å
α	90 deg
β	97.055(7) deg
γ	90 deg
Volume	4088.1(6) $Å^3$
Z	4
Calculated density	2.025 Mg/m^3
Absorption coefficient	27.548 mm^{-1}
Theta range for data collection	2.028 to 57.113 deg
Reflections collected / unique	20021 / 8068 [R(int) = 0.0795]
Completeness to theta = 53.594	100.0 %
Data / restraints / parameters	8068 / 777 / 401
Final R indices [I>2sigma(I)]	R1 = 0.1146, wR2 = 0.3028
R indices (all data)	R1 = 0.1326, wR2 = 0.3218
Goodness-of-fit on F^2	1.066

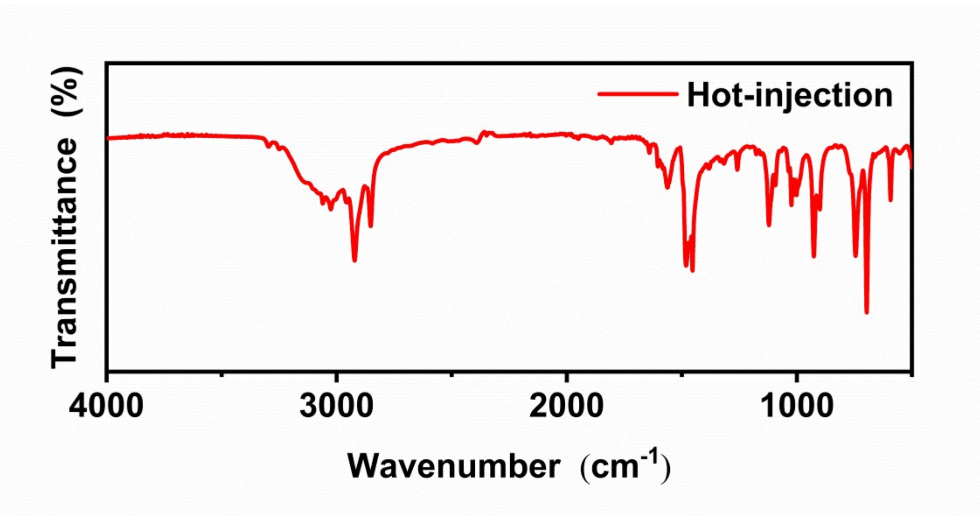

Figure S7. The FTIR spectrum of $(PEA)_4Cu_4I_4$ powder synthesized by the hot-injection method.

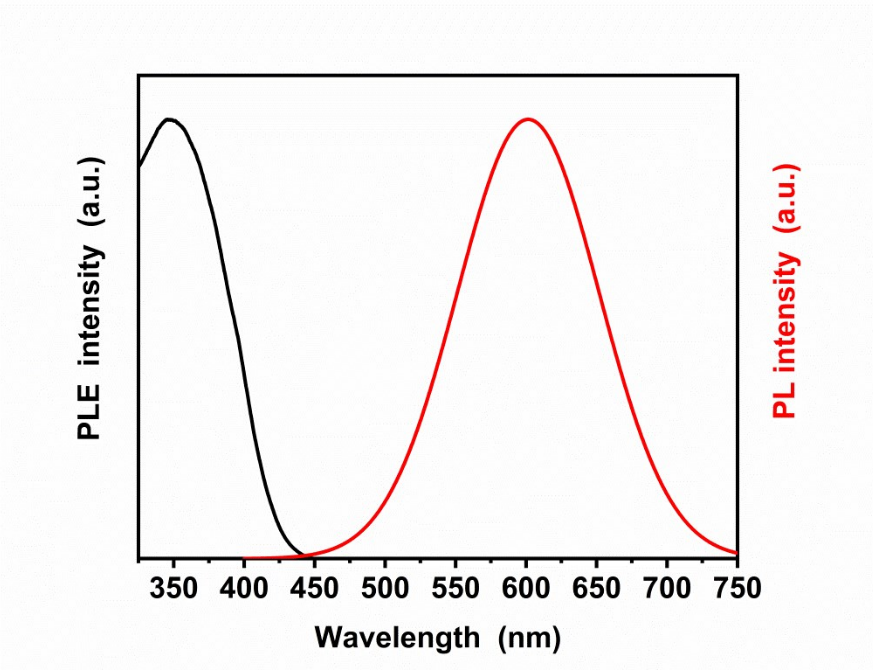

Figure S8. Excitation and emission spectrum of $(PEA)_4Cu_4I_4$ powder synthesized by the hot-injection method.

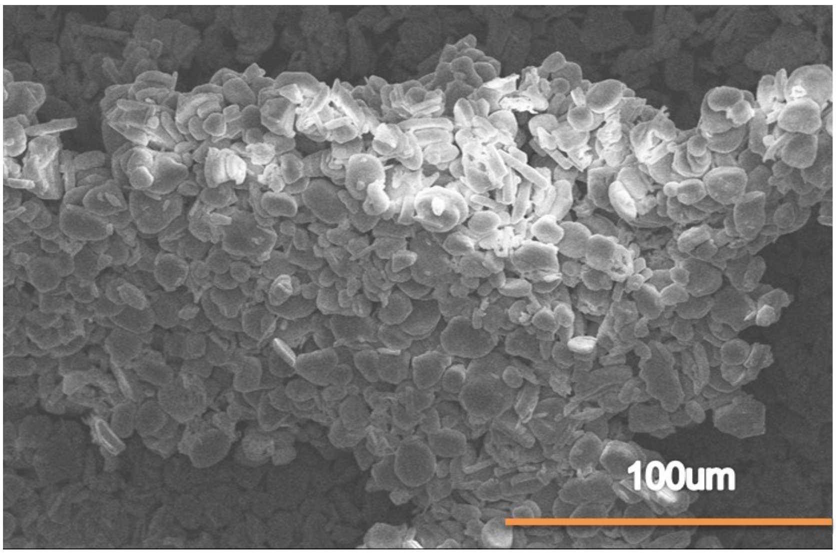

Figure S9. SEM image of $(PEA)_4Cu_4I_4$ powder synthesized by the hot-injection method.

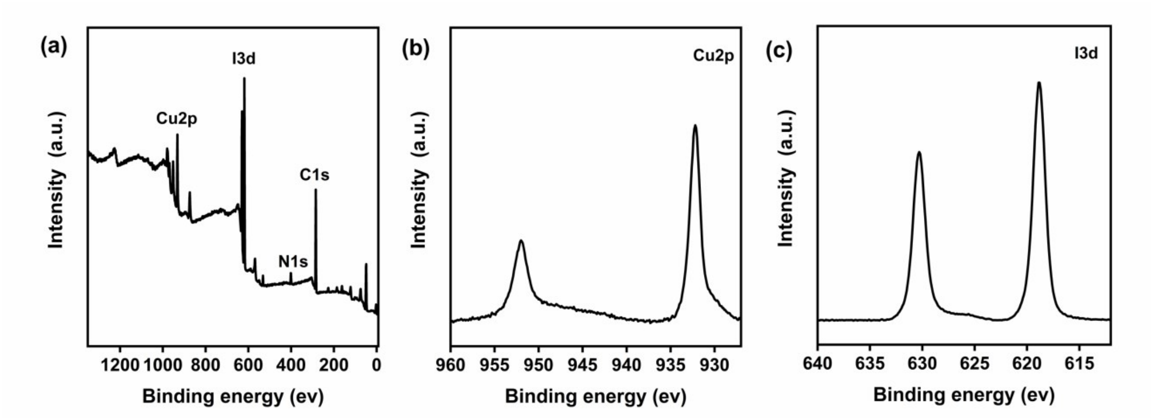

Figure S10. (a) Wide-scan XPS spectrum of $(PEA)_4Cu_4I_4$ powder synthesized by the hot-injection method. (b) and (c) XPS spectra of Cu 2p and I 3d, respectively.

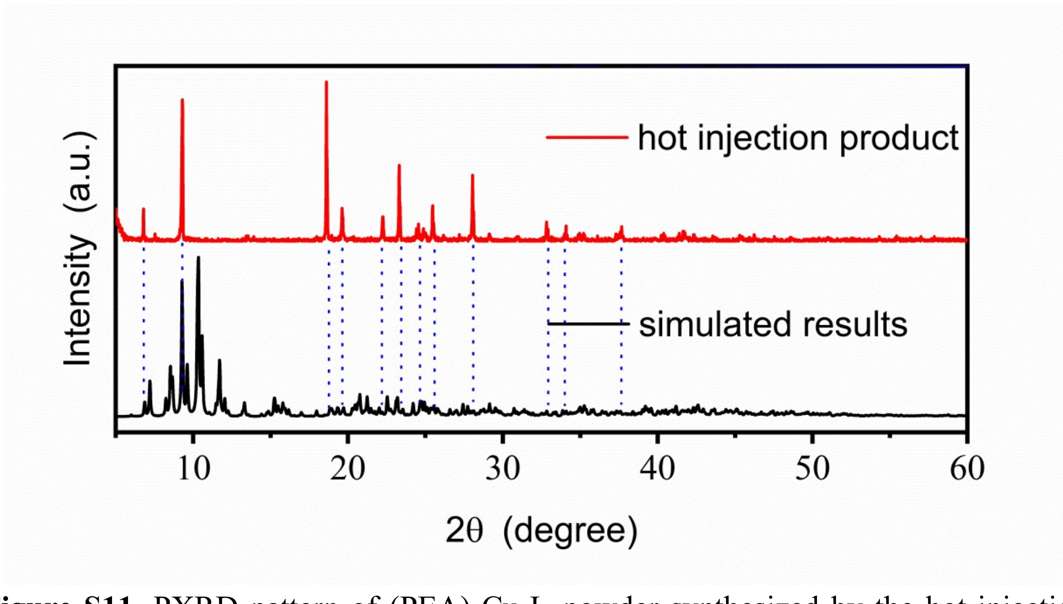

Figure S11. PXRD pattern of $(PEA)_4Cu_4I_4$ powder synthesized by the hot-injection method as well as the software simulation results (All the peaks of hot injection product are included in the simulated results and the different peak intensities demonstrate that the difference of crystal orientation).

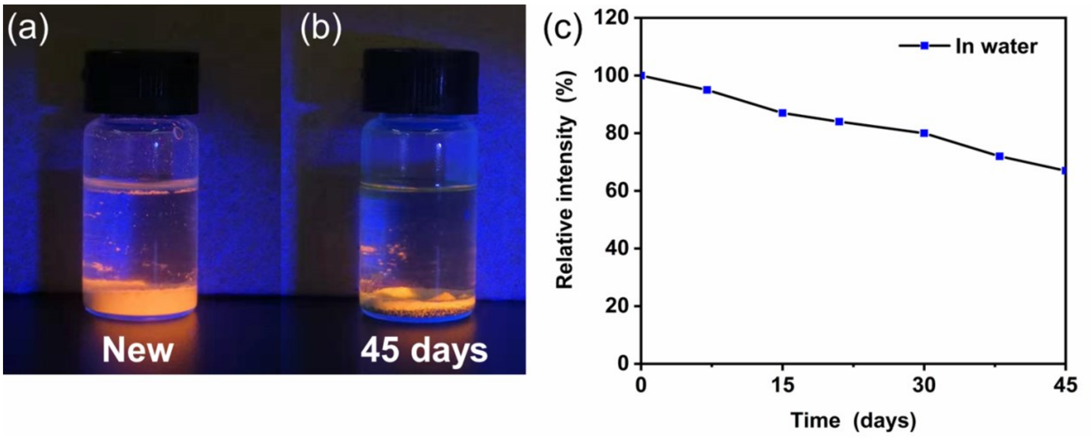

Figure S12. (a) Photograph of the $(PEA)_4Cu_4I_4$ powder synthesized by the hot-injection method at initial state in water under UV light. (b) Photograph of the $(PEA)_4Cu_4I_4$ powder synthesized by the hot-injection method at 45 days in water under UV light. (c) PL relative intensity of $(PEA)_4Cu_4I_4$ powder synthesized by the hot-injection method as a function of time in water.

References

1. Tard, C.; Perruchas, S.; Maron, S.; Le Goff, X. F.; Guillen, F.; Garcia, A.; Vigneron, J.; Etcheberry, A.; Gacoin, T.; Boilot, J.-P. Thermochromic Luminescence of Sol−Gel Films Based on Copper Iodide Clusters. *Chem Mater* 2008, 20, 7010-7016.
2. Xie, H.; Kinoshita, I.; Karasawa, T.; Kimura, K.; Nishioka, T.; Akai, I.; Kanemoto, K. Structure Study and Luminescence Thermochromism in Hexanuclear 6-Methyl-2-Pyridinethiolato Copper(I) Crystals. *J Phys Chem B* 2005, 109, 9339-9345.
3. Perruchas, S.; Le Goff, X. F.; Maron, S.; Maurin, I.; Guillen, F.; Garcia, A.; Gacoin, T.; Boilot, J.-P. Mechanochromic and Thermochromic Luminescence of a Copper Iodide Cluster. *J Am Chem Soc* 2010, 132, 10967-10969.
4. Liu, Z.; Djurovich, P. I.; Whited, M. T.; Thompson, M. E. Cu4I4 Clusters Supported by P∧N-type Ligands: New Structures with Tunable Emission Colors. *Inorg Chem* 2012, 51, 230-236.
5. Fu, W.-F.; Gan, X.; Che, C.-M.; Cao, Q.-Y.; Zhou, Z.-Y.; Zhu, N. N.-Y. Cuprophilic Interactions in Luminescent Copper(I) Clusters with Bridging Bis(dicyclohexylphosphino)methane and Iodide Ligands: Spectroscopic and Structural Investigations. *Chemistry – A European Journal* 2004, 10, 2228-2236.
6. Shan, X.-C.; Jiang, F.-L.; Yuan, D.-Q.; Wu, M.-Y.; Zhang, S.-Q.; Hong, M.-C. The unusual thermochromic NIR luminescence of Cu(i) clusters: tuned by Cu–Cu interactions and packing modes. *Dalton Trans* 2012, 41, 9411-9416.
7. Zink, D. M.; Baumann, T.; Friedrichs, J.; Nieger, M.; Bräse, S. Copper(I) Complexes Based on Five-Membered P∧N Heterocycles: Structural Diversity Linked to Exciting Luminescence Properties. *Inorg Chem* 2013, 52, 13509-13520.
8. Benito, Q.; Le Goff, X. F.; Nocton, G.; Fargues, A.; Garcia, A.; Berhault, A.; Kahlal, S.; Saillard, J.-Y.; Martineau, C.; Trébosc, J.; Gacoin, T.; Boilot, J.-P.; Perruchas, S. Geometry Flexibility of Copper Iodide Clusters: Variability in Luminescence Thermochromism. *Inorg Chem* 2015, 54, 4483-4494.
9. Zhang, X.; Liu, W.; Wei, G. Z.; Banerjee, D.; Hu, Z.; Li, J. Systematic Approach in Designing Rare-Earth-Free Hybrid Semiconductor Phosphors for General Lighting Applications. *J Am Chem Soc* 2014, 136, 14230-14236.
10. Fang, Y.; Liu, W.; Teat, S. J.; Dey, G.; Shen, Z.; An, L.; Yu, D.; Wang, L.; O'Carroll, D. M.; Li, J. A Systematic Approach to Achieving High Performance Hybrid Lighting Phosphors with Excellent Thermal- and Photostability. *Adv Funct Mater* 2017, 27, 1603444.
11. Liu, W.; Fang, Y.; Wei, G. Z.; Teat, S. J.; Xiong, K.; Hu, Z.; Lustig, W. P.; Li, J. A Family of Highly Efficient CuI-Based Lighting Phosphors Prepared by a Systematic, Bottom-up Synthetic Approach. *J Am Chem Soc* 2015, 137, 9400-9408.
12. Fang, Y.; Sojdak, C. A.; Dey, G.; Teat, S. J.; Li, M.; Cotlet, M.; Zhu, K.; Liu, W.; Wang, L.; ÓCarroll, D. M.; Li, J. Highly efficient and very robust blue-excitable yellow phosphors built on multiple-stranded one-dimensional inorganic–organic hybrid chains. *Chem Sci* 2019, 10, 5363-5372.
13. Hei, X.; Liu, W.; Zhu, K.; Teat, S. J.; Jensen, S.; Li, M.; O'Carroll, D. M.; Wei, K.; Tan, K.; Cotlet, M.; Thonhauser, T.; Li, J. Blending Ionic and Coordinate Bonds in Hybrid Semiconductor Materials: A General Approach toward Robust and Solution-Processable Covalent/Coordinate Network Structures. *J Am Chem Soc* 2020, 142, 4242-4253.
14. Kurkcuoglu, G. S.; Yesilel, O. Z.; Cayli, I.; Büyükgüngör, O. Synthesis, crystal structure, vibrational spectra and thermal properties of the cyano-bridged hetero-nuclear polymeric complex

$[Cd(pea)_2Ni(\mu\text{-}CN)_4]_n$. *Zeitschrift für Kristallographie - Crystalline Materials* 2009, 224, 493-498.